



Building optimal regime-switching portfolios

Vito Ciciretti ^a, Andrea Bucci ^{b,*}

^a Independent Researcher, Berlin, Germany

^b Department of Economics, Università degli Studi "G. d'Annunzio" Chieti-Pescara, Italy

ARTICLE INFO

JEL classification:

G10
G11
C58
C38
C61

Keywords:

Portfolio optimization
Portfolio construction
Regime-switching
Eigenvector centrality
Graph theory
Hierarchical clustering

ABSTRACT

This paper introduces a novel portfolio optimization method, the Clustered Minimum Spanning Tree Nested Optimization, capable of overcoming the limitations of classical asset allocation, such as instability and over-concentration of portfolio weights, and providing a defensive mechanism against the enhanced systematic risk during high-volatility periods. To do so, we follow a graph theory and clustering-based multi-step approach that accounts also for volatility regime switches. In a bootstrapping setup, we show that our approach produces well-diversified and stable portfolios outperforming the competing methods in terms of risk-adjusted performance while curtailing tail risk by achieving lower portfolio kurtosis.

1. Introduction

The classical Markowitz (1952) asset allocation model is the stronghold of portfolio construction since its first appearance in 1952. Over the years, however, extensive research documents three main limitations, namely producing unstable, over-concentrated, and underperforming portfolios, see Michaud (1989) for an in-depth analysis. The key step of the optimization process requires the estimation and the inversion of the covariance matrix of asset returns. As such, the standard error associated with the estimation propagates with the inversion and may cause the resulting portfolios to be unstable (Jobson & Korkie, 1980). Indeed, the higher the covariances among securities, the more likely the Markowitz approach is to return concentrated and unstable portfolios (Ledoit & Wolf, 2004). Moreover, this methodology is prone to underperform when diversification is most needed since covariances jump higher during market regimes characterized by high volatility (Preis et al., 2012).

To tackle Markowitz's pitfalls, Black and Litterman (1992) link the instability and concentration of Markowitz portfolios to the noisy estimate of expected returns by merging subjective return expectations with Capital Asset Pricing Model (CAPM) equilibrium returns. However, this approach does not deal with the noisily estimated covariance matrix and only reduces the ex-post instability of optimal portfolios. Clarke et al. (2002) propose to introduce stronger constraints to the convex optimization problem, such as long-only positions, market neutrality, and large-cap equities. Nevertheless, this approach leads to hefty modifications of the feasibility region, challenging portfolio performance. More recently, Lopez de Prado (2016b) introduces the Hierarchical Risk Parity (HRP) algorithm based on clustering the securities depending on the correlations among asset returns to avoid concentrated portfolios. Through this approach, similar investments are placed together, dissimilar investments are placed far apart, and optimal weights are equal to the inverse of the volatilities of the single stocks. Still, HRP employs a single linkage clustering to build the tree, which

* Correspondence to: Viale Pindaro, 42, Pescara, Italy.

E-mail address: andrea.bucci@unich.it (A. Bucci).

leads to a widened tree and results in an unequal distribution of the portfolio weights (Papenbrock, 2011). Despite this pitfall, Lopez de Prado's work is deemed as a cornerstone in the portfolio construction literature, and has attracted abundant attention to clustering strategies, such as the work by Raffinot (2017) for constructing portfolios through hierarchical clustering.

Relying on a different approach, Onnela et al. (2003) pioneer the application of graph theory to financial markets by studying the time-evolution of a Minimum Spanning Tree comparing calm periods with highly volatile ones as well as illustrating their hierarchical structure which allows improving asset clustering. In the same context, Peralta and Zareei (2016) prove how graph centrality measures are tightly related to optimal portfolio weights. Moreover, they build portfolios switching from a concentration in the core of the graph to the peripheries depending on a volatility threshold. However, in their work, the distinction between the core and peripheries depends on a static threshold, and the number of securities is rather arbitrary. Following their suggestion, Vÿrost et al. (2019) construct optimal portfolios based on four graphical representations of the securities: a complete graph, a minimum spanning tree, a planar maximally filtered graph and a threshold significance graph. Finally, Lopez de Prado (2016a) popularizes nested optimizations in portfolio construction. His Nested Clustered Optimization (NCO) algorithm first clusters the covariance matrix to compute the optimal allocations within each cluster with a convex optimization; then, the algorithm computes the optimal allocations between clusters by solving a second convex optimization and obtains overall optimal weights by combining the two optimizations.

Building upon Lopez de Prado (2016b) and Peralta and Zareei (2016), this article proposes the Regime-Switching Clustered Minimum Spanning Tree Nested Optimization (RS-CMSTNO) approach, which blends together hierarchical clustering and Minimum Spanning Trees (MST)¹ to build well-diversified portfolios that can timely react to regime switches and provide superior risk-adjusted performances. To our knowledge, this is the first study that combines the use of graph theory, eigenvectors centrality and regime-switching methods to build optimal portfolios.

RS-CMSTNO aims to overcome the three major limitations of the classical Markowitz approach. First, as in Lopez de Prado (2016a, 2016b), RS-CMSTNO aims at improving portfolio stability through denoising realized covariance matrices using the method proposed in Potters et al. (2005). Estimates of conditional covariances are inherently noisy, since they are an approximation of the true unobserved co-volatilities (see Patton, 2011). Hence, denoising covariance matrices results in less sensitive covariances to estimation errors. Second, RS-CMSTNO addresses portfolio concentration thanks to a nested optimization, as securities within the same hierarchical cluster are equally weighted in the within-cluster allocation step. Therefore, as long as the subsequent convex optimization assigns a non-zero weight to a cluster, all the securities therein receive a non-zero weight, too. Finally, moving to underperformance, RS-CMSTNO blends regime switches and eigenvector centrality into the quadratic optimization problem, with the former allowing higher returns as a consequence of more efficient portfolio rebalancing in response to changes in volatility regimes, and the latter allowing to control the degree of portfolio diversification. Specifically, in a high volatility regime we diminish the cross-security connectivity by allocating less weight in the graph's core, where eigenvector centrality is higher, and more on the peripheries of the graph, where eigenvector centrality is lower, hence resulting in a timely rebalancing of the portfolio. This allows alleviating the burden of systematic risk during periods of high volatility and taking advantage of periods of market growth in times of low volatility (which are associated with positive returns, especially in equity and fixed income markets, Haugen et al., 1991). In fact, in the graph theory literature, systemic risk shocks are referred to as abrupt changes in the density of cross-security connectivity (see Billio et al., 2012). The 2008 Global Financial crisis and the COVID-19 pandemic have shown how systematic shocks may quickly propagate across financial markets and cause substantial losses to portfolio managers. Therefore, incorporating regime switches into asset allocation problems can timely prompt the rebalancing of portfolios in response to exogenous events. For identifying regime switches, we use the Vector Logistic Smooth Transition Autoregressive model (VLSTAR) with a two-regime specification, as proposed in Bucci and Ciceretti (2022).

We compare the RS-CMSTNO portfolios with those produced by a CMSTNO without regime switches, the Hierarchical Risk Parity (HRP) approach (Lopez de Prado, 2016b), the Markowitz-based Maximum Sharpe ratio (MSR) and the Minimum Variance portfolio (MVP) methods. We cross-check the performance against a buy-and-hold strategy on the S&P500 implemented via the SPY exchange-traded fund. For a robust comparison, we use a bootstrapping approach that randomly selects a number of stocks out of the entire sample and iterates through ten-thousand simulations. With monthly rebalancing, results point to RS-CMSTNO producing well-diversified, stable portfolios outperforming the competing methods in terms of risk-adjusted performance while achieving lower portfolio kurtosis.

The rest of the paper is organized as follows. Section 2 states the classical portfolio optimization problem and explains the RS-CMSTNO here proposed. Section 3 introduces the dataset. Section 4 reports the bootstrapped results. Section 5 concludes.

2. Regime-switching clustered minimum spanning tree nested optimization

Let us consider N securities in a financial market with a vector of expected returns, μ . Let Σ be their $N \times N$ non-singular positive semi-definite covariance matrix, and r_f be the risk-free rate. The traditional (Markowitz, 1952) asset allocation method computes the optimal $N \times 1$ vector of weights w^* by solving the following convex optimization problem:

$$\begin{aligned} \min_w \quad & w' \Sigma w \\ \text{s.t.} \quad & w' \mu = c, \quad c \in \mathbb{R} \\ & w' \mathbf{1} = 1 \end{aligned}$$

¹ A Minimum Spanning Tree is a subset of graphs that has all the vertices covered with the minimum possible sum of edge weights.

where $w'1 = 1$ is the feasibility constraint of fully invested portfolios and c is the expected portfolio return. Therefore, the Lagrangian multiplier provides the optimal solution:

$$w^* = \frac{c - r_f}{q} \Sigma^{-1} (\mu - r_f 1) \quad (1)$$

where w^* is the optimal vector of weights, 1 is an N -dimensional vector of ones and $q = (\mu - r_f 1)' \Sigma^{-1} (\mu - r_f 1)$. The vector of returns and the covariance matrix (μ, Σ) in Eq. (1) need to be estimated. Given that their estimate is inherently noisy (see Patton, 2011), the inversion of the covariance matrix propagates the estimation error, resulting in unstable solutions wherein minor changes in the inputs cause extreme changes in the solution (Michaud, 1989). The instability of the covariance matrix is caused by both its noise and its signal (Lopez de Prado, 2016a). In fact, as the ratio between the number of assets N and the number of observations T is close to 1, the set of eigenvalues λ spans a wider range and since the smallest eigenvalues are closer to 0 as $\frac{N}{T} \rightarrow 1$, the determinant of $\hat{\Sigma}$ approaches zero and $\hat{\Sigma}^{-1}$ cannot be estimated robustly, hence leading to unstable solutions for w^* caused by the noise. The instability caused by the signal, instead, mostly arises during market downturns, when linear correlations jump higher. In this situation, the largest eigenvalues grow, hence the determinant of the matrix approaches zero, which in turn causes the inverse of the matrix to explode. There have been several proposals to adjust the estimation of the covariance matrices. Shrinkage methods mostly use a convex transformation to scale every eigenvalue (Ledoit & Wolf, 2003), yet these methods do not separate noise from the signal. For this reason, as further discussed in the next Section, we use the method proposed by Potters et al. (2005).

2.1. Returns and denoised covariance matrix

Starting from the time-series of security prices, we first calculate hourly log-returns as:

$$r_{i,\tau} = \ln \left(\frac{p_{i,\tau}}{p_{i,\tau-1}} \right) \quad \forall \tau = 1, \dots, n_t,$$

where $p_{i,\tau}$ is the price of the i th asset at time τ , with $i = 1, \dots, N$, and n_t is the number of hours in the t th month for $t = 1, \dots, T$, thus $r_t = [r_{1,\tau}, \dots, r_{N,\tau}]'$ is the $N \times 1$ vector of asset returns.

We then calculate the return covariance matrix which will be used to obtain the adjacency matrix for the construction of the minimum spanning tree. Barndorff-Nielsen and Shephard (2004) show that return covariances can be estimated through the non-parametric realized covariances, RC_t , which converge in probability to the quadratic covariation of the prices' process under very general assumptions. Following De Pooter et al. (2008) and Liu (2009), we calculate monthly realized covariances, RC_t , as the aggregation of cross-products of hourly returns and overnight volatility, such that:

$$RC_t = \sum_{\tau=1}^{N_t} r_{\tau,t} r'_{\tau,t} + \sum_{j=1}^J rco_{i,t} rco'_{i,t} \quad (2)$$

where N_t is the number of hourly observations in the t -month, for $t = 1, \dots, T$ and r_τ is the $n \times 1$ vector of asset returns for the τ th observation and rco_j is the $n \times 1$ vector of close-to-open returns from day j to day $j + 1$. This ensures positive definite realized covariance matrices and makes volatility fully observable and mouldable with any time series model. However, when data are collected at high-frequencies, microstructure errors may arise (Andersen et al., 2000; Zhou, 1996). For this reason, we also apply our methodology when the returns covariance matrix is estimated through the flat-top realized kernel estimator by Barndorff-Nielsen et al. (2006), computed as follows

$$RCK_t = \hat{\gamma}_0 + \sum_{s=1}^h \omega_s (\hat{\gamma}_s + \hat{\gamma}_{-s}), \quad (3)$$

where $\hat{\gamma}_s = \sum_{i=1}^{N_t} r_i r_{i-s}$, with $s = -h, \dots, h$ where h is size of the sample window, $\omega_s = k\left(\frac{s-1}{h}\right)$ and k is a function taking values between 0 and 1, such that $k(0) = 0$ and $k(1) = 0$.

Once obtained the realized covariance matrix as in Eqs. (2) and (3), we denoise it following the Constant Residual Eigenvalue method (Potters et al., 2005), yielding matrices with a lower condition number. The main idea behind denoising the covariance matrix is to eliminate the eigenvalues that represent noise. Denoised covariance matrices are not only useful to tackle the aforementioned instability of the convex problem, but also to determine meaningful clusters with denoised distance metrics.

2.2. Clustering the minimum spanning trees

In the next step, we convert the covariances into adjacency matrices to topologically arrange the securities into Minimum Spanning Trees (MST) and then cluster upon them. In fact, covariance matrices lack the notion of hierarchy. Simon (1991) argues that complex systems, such as financial markets, can be arranged in a natural hierarchy comprising nested substructures. The lack of hierarchical structure makes portfolio weights vary in unintended ways (Lopez de Prado, 2016b). Moreover, the goal of codependence analysis is choosing which cross-security dependencies matter. From a tree representation standpoint, this means choosing which links in the tree are significant while pruning non-significant relationships. For this reason, the MST representation is particularly useful in financial applications, being the subset of a graph including all the vertices (e.g. securities) connected by the minimum possible number of links. In fact, in line with Onnela et al. (2003), we believe that Minimum Spanning Trees –

being a pruned representation of asset correlation – offer a robust and descriptive representation of financial markets. Moving from covariance matrices to Minimum Spanning Trees, we have effectively pruned the system from a $N(N-1)/2$ to $N-1$ elements of information. This allows the introduction of a hierarchical structure, where the relationship among securities is quantifiable by means of centrality measures. In turn, the hierarchical property resembles the traditional dichotomy of systematic and idiosyncratic risk differentiated by the geometrical displacement of securities between the core of the tree and peripheries.

The approach starts with building the adjacency matrix to represent the links between securities in the tree. Each entry indicates whether pairs of securities are adjacent. However, since clustering requires a distance measure that satisfies the three axioms of a Euclidean metric, before forming the adjacency matrix we shall transform the covariances into metrics. As described in Mantegna (1999), the procedure foresees the transformation of the denoised covariances, $\sigma_{i,j}$, in denoised correlations as $\rho_{i,j} = \sigma_{i,j}/\sigma_i\sigma_j$, where σ_i is the i th standard deviation, $\forall i, j$, and then into metrics, such that $d_{i,j} = 1 - \rho_{i,j}^2$. The diagonal of the adjacency matrix is set equal to zero to avoid self-loops². A non-zero entry in the adjacency matrix indicates the existence of a financial relationship (direct or inverse) between pairs of securities where the strength of the link is measured by $d_{i,j}$. Although this measure neglects the sign of the correlation coefficient, as the square function does not allow distinguishing two correlations of equal value but with different signs, this has a twofold advantage. First, the obtained distances are Euclidean metrics, hence they can be passed as input to a clustering algorithm. Second, it embeds the simple intuition that the correlation between two securities is proportional to the topological distance between securities in a topological space.

Once formed the adjacency matrix, we build the minimum spanning tree. Consider a graph $G = (V, L, W)$ formed by a finite set of N nodes of vertices V , a set of directed links $L \subset V \times V$, where each $(x, y) \in L$ represents a link from $x \in V$ to $y \in V$, and a set of positive weights $W : L \rightarrow \mathbb{R}_{++}$ defined on each link. A spanning tree is a connected, undirected subgraph of G where all the nodes are connected by the respective link set.³ The Minimum Spanning Tree of a weighted graph is a minimum weight spanning tree, $S \subseteq L$, that among all the spanning trees of G solves:

$$\min_S \sum_{l \in S} W(l)$$

where $S \subseteq L$ is the number of links in the MST and l represents each link in each realization, s , of S .

To calculate the Minimum Spanning Tree, we employ the algorithm by Kruskal (1956). Starting from a tree in each vertex, Kruskal's algorithm removes any link with a minimum weight between the vertices, combining the trees for which the link has been removed.

The MST representation allows quantifying the influence structure among the securities by means of a centrality measure. A centrality measure $C : V \rightarrow \mathbb{R}_+$ is a function that assigns a non-negative value to each node such that the higher the value, the more the node is central. As such, peripheral nodes that have a limited impact on the dynamics of the network have lower centrality, while higher centrality nodes play a major role. In our methodology, we use the eigenvector centrality measure, according to which a security displays a high centrality either by direct links to other securities or by being connected to other securities that are themselves highly central. In fact, the eigenvector centrality ζ of each node x is given by the weighted average of the centrality values of its neighbors, x' :

$$\zeta(x) := \frac{1}{\lambda} \sum_{(x,x') \in L} W(x, x') \zeta(x') \quad (4)$$

where λ is a constant (see Bollobás, 1998a, Chapter 8, Theorem 5, for further details). Within the MST representation, securities that have stronger connections to several other securities, typically placed at the core of the tree, display a high level of eigenvector centrality. Securities in the peripheries display lower eigenvector centrality values, mirroring the fewer, less intense connections to the rest of the market. We use eigenvector centrality to control portfolio concentration in response to detected market regimes. When a transition to a high-volatility regime is spotted, our method builds a portfolio with a lower eigenvector centrality to steer away from market risk and focus on the peripheries, where returns are more driven by idiosyncratic factors. Having a higher portfolio eigenvector centrality during calm market regimes, instead, allows the portfolio to grow in line with the overall market. Therefore, eigenvector centrality enters in the optimization problem as a constraint strictly depending on the probability of being in a high volatility regime.

The MST representation is also useful for clustering the securities and, possibly, avoiding portfolio concentration. Specifically, we partition the vertices into K clusters by means of the Agglomerative Nesting (AGNES) algorithm (Kaufman & Rousseeuw, 1990) with a Manhattan distance and the Ward linkage function (Ward, 1963) and obtain K clusters of securities. To calculate the optimal number of clusters K we use the gap statistic introduced by Tibshirani et al. (2001).

2.3. Within-cluster weights

With the securities partitioned into K clusters, RS-CMSTNO assigns a preliminary set of within-cluster weights by equally weighting the securities within the same cluster,

$$w_{wi,k} = \frac{1}{N_k}, \quad k = 1, \dots, K \quad (5)$$

² A self-loop is a link that connects a vertex to itself. We eliminate self-loops since self-relations are insignificant in portfolio construction.

³ For a general introduction to graph theory, see Bollobás (1998b, 2001).

where $w_{wi,k}$ is a $N_k \times 1$ vector of equal weights, $w_{wi} = [w_{wi,1}, \dots, w_{wi,K}]'$ is the $N \times 1$ vector of within-cluster weight, N_k is the number of securities in each cluster, and K is the number of clusters. Choosing equal weighting simplifies the first part of the optimization and allows the optimal allocation of resources guaranteeing a minimum investment in each security within a cluster, hence leaning towards less concentrated portfolios. In fact, securities belonging to the same cluster are exposed to the same amount of systematic risk (we disregard idiosyncratic risk). High-frequency portfolio rebalancing may result in high transaction costs, assuming that fees are charged proportionally to the number of new transactions, rather than volumes. Nevertheless, our results concern monthly rebalancing, thus limiting transaction costs while closely matching the real-life rebalancing strategies of portfolio managers. Finally, Hierarchical Risk Parity – as most of the asset allocation methodologies focused on systematic risk, such as risk parity – results in assigning a non-zero weight to all the securities in the portfolio. As such, an inherent trade-off arises between tackling the over-concentration issue of Markowitz's portfolios against minimizing the transaction costs.

2.4. Between-cluster and final weights

All that is left now is calculating between-cluster weights and combining them with the within-cluster ones to obtain the final portfolio weights. In this step, the focus switches to clustered quantities. To do so, our method foresees the computation of aggregated returns, covariances, and eigenvector centralities at a cluster level. To estimate the clustered covariance matrix, we use sample covariance matrices calculated on a T -dimensional rolling-window.⁴ Aggregated returns and eigenvector centralities are computed as equally weighted average within each cluster. Centrality measures can enter the optimization process either as a target or a constraint. As in [Výrost et al. \(2019\)](#), we include eigenvector centrality as a constraint in the convex optimization process. As for the portfolio mean return, a scalar portfolio eigenvector centrality value – obtained via linear aggregation across securities – is passed as the target. Our approach, instead, differs from [Peralta and Zareei \(2016\)](#) as in the latter eigenvector centrality is used to build an equally weighted portfolio which only invests in the securities displaying the highest values.

This step also introduces market regimes for the calculation of between-cluster weights. Incorporating market regimes allows to timely rebalance the portfolio in response to regime switches, seizing positive performance against other non-regime-switching portfolio construction methodologies. To detect regimes, we apply the methodology described in [Bucci and Ciciretti \(2022\)](#), which employ the Vector Logistic Smooth Transition Autoregressive model (VLSTAR), defined as in [Anderson and Vahid \(1998\)](#). The VLSTAR model is applied to the first principal components of the half-vectorization of realized covariance matrices (*i.e.*, we consider only the elements belonging to the lower triangular portion of the covariance matrix) that explain at least 75% of the variance. Since the half-vectorization stacks realized covariances in a $N(N+1)/2 \times 1$ vector for each t , dimensionality reduction through the use of principal components is necessary for the convergence of a nonlinear complex model, such as VLSTAR. The choice of the transition variable, crucial for the definition of the logistic function, is made upon the lagged principal components selected.

The value of the logistic function is then used to scale the clustered eigenvector centrality and reformulate the traditional convex optimization problem, and calculate the $K \times 1$ vector of between-cluster weights such that:

$$\begin{aligned} \min_{w_b} \quad & w_b' \hat{\Sigma}_k w_b \\ \text{s.t.} \quad & w_b' \hat{\mu}_k = q \\ & w_b \cdot \hat{\zeta}_k = \frac{u}{\eta(1+p)}, \quad q, u, \eta \in \mathbb{R} \\ & w_b' \mathbf{1} = 1 \\ & w_b \geq 0 \end{aligned}$$

where the subscript k refers to clustered quantities, ζ_k represents the cluster eigenvector centrality, q and u are the targeted scalar values for the mean and eigenvector centrality aggregated linearly across the portfolio weights, μ_k is the cluster mean return, p is the value of the logistic function and η is a scalar parameter that controls its weight.⁵ The latter is calibrated via grid-search and can be seen as the sensitivity of the portfolio to regime switches, resembling the inverse of the investor's degree of risk aversion. The novelty of our approach is represented by the constraint $w_b \cdot \hat{\zeta}_k = \frac{u}{\eta(1+p)}$. As $p \rightarrow 1$, $\zeta_k \rightarrow \frac{u}{2\eta}$, it follows that the higher the probability of being in a high volatility regime, the lower the target eigenvector centrality, as well as the portfolio concentration. As such, when observing a higher probability of being in a high volatility regime, the portfolio rebalances to ensure a higher degree of diversification, which under the MST representation is achieved by lowering the portfolio eigenvector centrality. A non-regime-switching CMSTNO approach can be obtained by setting $\eta = 1$ and $p = 0$. In RS-CMSTNO, we also add the constraints of fully invested portfolios ($w_b' \mathbf{1} = \sum_{k=1}^K w_b = 1$, where $\mathbf{1}$ is a vector of ones) and long-only positions ($w_{b,k} \geq 0$, for $k = 1, \dots, K$). We then compute the flattened N -dimensional vector of weights, \tilde{w}_b , by imputing the k element of w_b to all the N_k securities belonging to the k th cluster.

Finally, the portfolio weights, w^* , can be calculated as the Hadamard product of within-cluster, w_w , and flattened between-cluster weights, \tilde{w}_b , such that:

$$w^* = w_w \odot \tilde{w}_b \quad (6)$$

⁴ We leave out the first T^* temporal observations, where $T^* \in \mathbb{N}$ is a scalar input. One should set $T^* > N$ to yield a matrix with a rank larger than the number of assets, as $T^* < N$ would result in $(N - T^*) > 0$ zero eigenvalues ([Potters et al., 2005](#)).

⁵ All quantities refer to a specific period t , but we omit the temporal subscript for easing the notation.

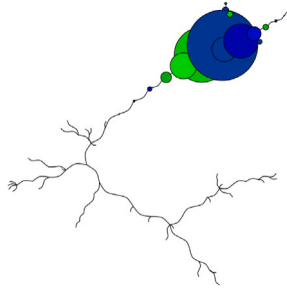


Fig. 1. MST in low volatility regime.

Note: The MST representation of the 100 largest US securities by market cap as of December 2019 (when the regime detection model signaled a low volatility regime). The structure of the tree appears stretched on four major sections, with the core of the tree placed at the top (the size of the vertices represent each asset's eigenvector centrality, wherein each node represents a security).

where \circ represents the Hadamard product. Noticeably, the sum of the weights in $w^* = (w_1^*, \dots, w_N^*)'$ is equal to 1, as well as $w_i^* \geq 0, \forall i = 1, \dots, N$, given that the equal weighting scheme preserves the fully invested and long-only constraints of the convex optimization.

3. Data and empirical application

The dataset used to assess the validity of our approach comprehends the time-series of hourly open spot prices of the 100 largest US stocks by market capitalization (as of September 2021) belonging to the S&P500 for the period January 2010–September 2021, sourced from Bloomberg (19,550 hourly observations). The starting date is chosen to neatly separate the ongoing, low-interest-rate investment phase from the preceding one. [Appendix A](#) reports the complete list of stock names and tickers. Asset returns are calculated on all hourly prices in a month. This means that we are covering overnight prices when we compute the return between the close price of a day and the open price of the following day. We calculate the monthly realized covariances as in both (2) and (3), yielding 142 monthly observations. Choosing a monthly aggregation for the cross-products implies that the portfolios are rebalanced at a monthly frequency.

Focusing on the inspection of the MST on the whole sample of one-hundred stocks, [Figs. 1](#) and [2](#) allow a comparison of the MST representation during a single month in a low-volatility regime (December 2019) and in a high volatility regime (March 2020) respectively. Each node represents a security, while the size of each node is proportional to its eigenvector centrality (the color in the Figure is chosen randomly and serves aesthetic purposes only). As it is visible, the MST at the onset of the COVID-19 crisis presents a denser structure where the connections between the securities are stronger. For this reason, a regime-switching procedure that is capable of timely rebalancing the portfolio when a switch to a high volatility regime is spotted can greatly enhance portfolio performance by timely increasing the degree of diversification. In graph terms, the approach would allocate higher weight to the peripheries of the graph (*i.e.*, the four branches with smaller vertices) further away from the dense core wherein the enhanced systemic risk increases the connection between the securities and challenges the portfolio performance. In the [Appendix B](#), we report also the Figure in the low-volatility regime with tickers on the nodes to understand if MST puts together assets from the same sector. The MST reported in [Fig. B.3](#) shows that the topological representation yields clusters of stocks at industry level in a low volatility regime. In fact, MST renders the property of grouping together similar stocks, while placing further apart more dissimilar ones, based on the distance measure that has been employed to build the adjacency matrix. During high volatility regimes, instead, covariances tend to jump higher together, hence stocks become more similar amongst each other, at least in terms of negative performance. Hence, in volatile periods, the MST does not form in industry clusters, rather, becomes denser as the interconnectivity among stocks increases — pushing the whole market downwards, with the expectation of few stocks placed at the peripheries, whose value is rather driven by idiosyncratic shocks. Looking at the graph, at the core of the graph are placed most of the technology stocks, namely: AAPL, GOOGL, AMD, ADBE, CRM and NFLX. A second cluster of technology stocks is present at the left-hand side of the periphery, namely: QCOM, INTC, INTU, ADP, FISV, TXN. Consumer staples are also mainly present in the core of the tree, namely: KO, PEP, MDLZ, GIS, MO and PG. Pharma stocks are placed on the top branch of the periphery, namely: MRK, PFE, JNJ, AMGN, LLY, ABT, TMO, BDX, MDT, SYK, BDMY and GILD. For the energy sector, CVX and XOM are neighbors on the left-hand side. AMT, CCI and PLD, three stocks belonging to the real estate sector, are close to each other in the core of the tree. Consumer discretionary stocks are instead placed in the middle: AMZ, NKE, TJX, HD and LOW. Finally, financials are in the middle as well, on a branch below the one of consumer discretionary: UBS, AXP, C, GS, JPM, MS, WFC, BLK, BAC and SCHW.

Regime detection foresees the definition of the number of regimes and the choice of the transition variable used in the VLSTAR model. In accordance with a part of the literature on volatility regimes ([Bucci & Ciciretti, 2022](#); [Cho & White, 2007](#); [Davies, 1987](#); [Hansen, 1992](#)), we hypothesize two market regimes, *i.e.*, low volatility and high volatility. Therefore, the VLSTAR with 2 regimes is applied to the first three principal components (which explain in most of our samples more than 75% of the total variance) of the half-vectorization of the realized covariance matrices, which are then used as dependent variables. We choose to use the lagged first principal component as a transition variable throughout all the bootstrap sampling.

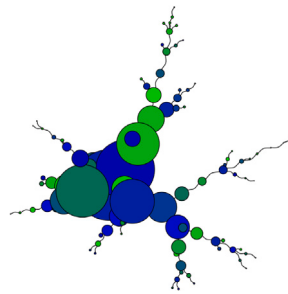


Fig. 2. MST in high volatility regime.

Note: The MST representation of the 100 largest US securities by market cap as of March 2020 (when the S&P 500 index hit its deepest point as a consequence of the COVID-19 crisis). The vertices of the tree (representing each security with size proportional to each asset's eigenvector centrality) present a dense structure with high values of eigenvector centrality recorded by most of the securities at the core of the tree. The interconnectivity among securities, together with the eigenvalues of the covariance matrix on which the adjacency matrix is built, bounced higher as a consequence of increased market risk.

4. Performance evaluation

We compare the Clustered Minimum Spanning Tree Nested Optimization procedure to the Hierarchical Risk Parity (HRP) of [Lopez de Prado \(2016b\)](#), the Markowitz-based Maximum Sharpe ratio (MSR) and the Minimum Variance portfolio (MVP) methodologies. To further highlight the benefits of the regime-switching methodology, we add the non-regime-switching CMSTNO – by setting $\eta = 1$ and $p = 0$ – to the comparison. We start with an assessment of the portfolio stability and concentration, to then analyze the performances in terms of risk-adjusted measures, namely Sharpe ratio, Sortino ratio, Information ratio and Treynor ratio. We assume portfolios are rebalanced on a monthly basis. Also, we detect the regimes on a monthly basis for the regime-switching specification. In fact, [Bucci and Ciceretti \(2022\)](#) argue that using higher detection frequencies identifies too recurrent switches as, for developed equity markets, the underlying return process converges to the monthly unconditional mean. As such, we shall not deem the mean reversion process characterizing the asset returns as a structural break. Finally, we estimate the scale parameter for the RS-CMSTNO approach, η , by means of grid search on the whole dataset of one-hundred stocks for which we obtained an optimal value of 0.85.⁶

To obtain a robust performance evaluation, we employ a bootstrapping approach. To do so, we use a bootstrapping application that in each run implements the portfolio construction strategy by selecting (without replacement) $n = 30$ stocks out of the entire sample of one-hundred stocks. We choose to iterate the process through 10,000 runs to collect sufficient observations to draw conclusions based on asymptotic convergence while minding computational complexity. In all simulations, we assume monthly rebalancing to match the best practice implemented by most mutual funds and minimize the impact of transaction costs. The bootstrapping setup is employed to check the robustness of portfolio performances in terms of stability, concentration, and performance of each optimal portfolio.

To measure portfolio stability, we use the turnover rate introduced by [DeMiguel et al. \(2014\)](#), according to which stable portfolios produce lower turnovers. Let us define the portfolio turnover rate as:

$$TO_t = \sum_{i=1}^N \left| w_{i,t+1} - w_{i,t} \frac{1 + r_t^i}{1 + w_{i,t} r_t^i} \right|$$

where w_t^i is the weight for the i th security in an N -dimensional vector of weights at time t and r_t^i is the return for the i th security in the portfolio. Essentially, at the end of each month t , an investor rebalances the portfolio using the ex-post covariance matrix to calculate the weights w_{t+1}^i for the next period. The moment before rebalancing the portfolio according to the new weights, the notional value of each security i changes to $w_t^i (1 + r_t^i)$ while its realized weight w_t^i becomes $w_t^i \frac{1 + r_t^i}{1 + w_{i,t} r_t^i}$. As a result, the portfolio turnover can be interpreted as the fraction of the portfolio being bought or sold at time t . As such, lower turnover values correspond to higher portfolio stability.

Moving to the measurement of the portfolio concentration, we use the Hirschman–Herfindahl Index (HHI) ([DeMiguel et al., 2014](#)). We define the concentration of a portfolio as the measure of inequality relative to the weight allocation of the available wealth among the available securities. Let us define the HHI index as the sum of squared weights:

$$HHI_t = \sum_{i=1}^N (w_{i,t})^2, \quad t = 1, \dots, T$$

where $w_{i,t}$ is the weight for the i th security in an N -dimensional vector of weights at time t . For fully invested portfolios, we have that $HHI_t \in \left[\frac{1}{N}, 1 \right]$. In this setting, an equally weighted portfolio records the smallest concentration, while a portfolio fully invested

⁶ The grid approach targets the maximization of the Sharpe ratio and extends from 0.05 to 1.5 with steps of (equal) size 0.05.

Table 1
Descriptive statistics of the turnover rate and the Hirschman–Herfindahl Index (HHI).

Normalized turnover rate				
Method	Mean	Median	1st quartile	3rd quartile
MVP	0.782	0.812	0.715	0.964
MSR	0.855	0.908	0.784	0.982
HRP	0.391	0.363	0.135	0.634
RS-CMSTNO	0.318	0.317	0.245	0.384
CMSTNO	0.276	0.265	0.195	0.350
Adjusted HHI				
Method	Mean	Median	1st quartile	3rd quartile
MVP	0.223	0.205	0.059	0.312
MSR	0.324	0.279	0.019	0.382
HRP	0.008	0.009	0.002	0.009
RS-CMSTNO	0.005	0.004	0.003	0.006
CMSTNO	0.004	0.003	0.002	0.005

Note: The descriptive statistics related to adjusted HHI and normalized portfolio turnover for each portfolio strategy. In boldface, we highlight the best performing method.

Table 2
Descriptive statistics of the turnover rate and the Hirschman–Herfindahl Index (HHI) when the covariance matrix is estimated with the realized kernel estimator.

Normalized turnover rate				
Method	Mean	Median	1st quartile	3rd quartile
MVP	0.771	0.793	0.743	0.925
MSR	0.793	0.888	0.783	0.966
HRP	0.311	0.323	0.131	0.583
RS-CMSTNO	0.328	0.302	0.235	0.363
CMSTNO	0.256	0.272	0.196	0.331
Adjusted HHI				
Method	Mean	Median	1st quartile	3rd quartile
MVP	0.163	0.129	0.055	0.285
MSR	0.231	0.218	0.021	0.311
HRP	0.004	0.006	0.002	0.008
RS-CMSTNO	0.002	0.004	0.001	0.006
CMSTNO	0.004	0.003	0.002	0.005

Note: The descriptive statistics related to adjusted HHI and normalized portfolio turnover for each portfolio strategy when the covariance matrix is estimated with the realized kernel estimator. In boldface, we highlight the best performing method.

in a single asset records an HHI of 1. As such, lower HHI values correspond to lower portfolio concentration. For better comparison across methodologies, we normalize the HHI as:

$$HHI_t^{(adj)} = 1 - \frac{1 - HHI_t}{1 - N^{-1}}$$

where the normalization yields $HHI_t^{(adj)} \in [0, 1]$.

Tables 1 and 2 report the summary statistics for both the normalized portfolio turnover and the adjusted HHI, respectively for RC calculated as in (2) and (3). The results have been averaged across the bootstrapped samples. In both the tables and for both statistics, CMSTNO portfolios have the lowest mean and median values. Compared to the HRP method, this exhibits a higher mean compared to the CMSTNO procedures, as in the latter the mechanism according to which each security receives a non-zero weight introduces major stability and a lower degree of concentration. Finally, MSR and MVP portfolios record the highest turnover and concentration across the different covariance estimation methods.

Finally, we compare the portfolios in terms of averaged risk-adjusted performance – namely via Sharpe ratio, Sortino ratio, Information ratio and Treynor ratio – as well as we analyze the descriptive statistics of their returns. For this section, we add to the comparison a buy-and-hold strategy on the S&P500 via the SPY exchange-traded fund (ETF). We disregard transaction costs as investors face heterogeneous fees, as a strategy can be implemented via different brokers and instruments (cash, futures, ETFs, etc.). Nevertheless, the monthly rebalancing frequency limits the portfolio turnover, thus curtailing the impact of transaction costs.

Results are reported in Tables 3 and 4. Interestingly, the results from the different estimation methods for RC are mostly overlapping, meaning that the goodness of our approach is not influenced by the estimation method of the return covariance matrix. The RS-CMSTNO and CMSTNO methodologies achieve the highest annualized mean return of 14.65% and 13.92% in Table 3, and 14.96% and 14.07% in Table 4. The regime-switching property is mirrored in higher average returns and lower volatility compared to the non-switching version. All the asset allocation techniques are effective in reducing the volatility of the investment portfolio compared to the buy-and-hold strategy. In particular, the MVP exhibits the lowest portfolio standard deviation. Moreover, CMSTNO

Table 3

Annualized performance for monthly rebalancing.

Method	Mean	St. dev.	Skew.	Kurt.	SR	Sortino	Info	Treynor
RS-CMSTNO	14.65%	13.31%	-1.29	2.45	0.80	1.42	4.81	0.98
CMSTNO	13.92%	14.24%	-1.54	2.54	0.82	1.38	4.34	0.95
HRP	10.52%	10.76%	-1.46	3.21	0.64	1.19	3.89	0.91
MSR	2.85%	10.84%	-0.64	4.05	0.53	0.58	1.29	0.69
MVP	3.02%	10.24%	-0.58	3.20	0.59	0.71	1.83	0.73
SPY	13.54%	16.06%	-0.94	5.01	0.85	1.12	2.9	0.85

Note: Values in boldface denote the best performing method for that measure. The first two columns refer to annualized mean and standard deviation of portfolio returns. 'Skew.' refers to the portfolio skewness, 'Kurt.' refers to the excess kurtosis with respect to a Normal distribution. The last four columns refer to the Sharpe ratio, Sortino ratio, Information ratio and Treynor ratio respectively.

Table 4

Annualized performance for monthly rebalancing and covariance estimated with realized kernel estimator.

Method	Mean	St. dev.	Skew.	Kurt.	SR	Sortino	Info	Treynor
RS-CMSTNO	14.96%	13.13%	-1.39	2.93	0.86	1.46	4.78	0.99
CMSTNO	14.07%	14.27%	-1.54	3.21	0.82	1.39	4.34	0.95
HRP	11.43%	11.47%	-1.38	3.85	0.64	1.20	3.89	0.92
MSR	3.23%	10.25%	-0.63	3.67	0.53	0.56	1.27	0.69
MVP	3.20%	9.25%	-0.56	3.34	0.57	0.72	1.84	0.74
SPY	13.54%	16.06%	-0.94	5.01	0.85	1.12	2.9	0.85

Note: Values in boldface denote the best performing method for that measure. The first two columns refer to annualized mean and standard deviation of portfolio returns. 'Skew.' refers to the portfolio skewness, 'Kurt.' refers to the excess kurtosis with respect to a Normal distribution. The last four columns refer to the Sharpe ratio, Sortino ratio, Information ratio and Treynor ratio respectively.

and RS-CMSTNO show higher volatility because of the equal weighting scheme that allocates a non-zero, minimum weight to each security within each cluster. The RS-CMSTNO achieves the lowest kurtosis in both the tables, proving its efficacy as hedge against tail risk events. Looking at the risk-adjusted measures, RS-CMSTNO is the best performing across all metrics. The HRP outperforms the buy-and-hold strategy. MSR and MVP, instead, exhibit the lowest returns as well as the worst risk-adjusted performances. We conclude that superior risk-adjusted returns are associated with diversifying away the systematic risk – a property shared by RS-CMSTNO, CMSTNO and HRP – as well as with shifting the allocation towards the peripheries of the MST by scaling the target portfolio eigenvector centrality with the output of a regime-detection procedure.

5. Conclusions

This paper aims at proposing a portfolio construction method that overcomes the limitations of the classical convex optimization-based methodologies, namely producing poorly diversified portfolios with unstable weights and underperforming returns, additionally requiring higher turnovers for the rebalancing activity. To address these limitations, we introduce a graph-theory-based method, the Regime-Switching Clustered Minimum Spanning Tree Nested Optimization (RS-CMSTNO), to calculate optimal regime-switching, fully invested portfolios based on a multi-step approach.

We compare the RS-CMSTNO to CMSTNO (*i.e.*, when the regime-switching property of RS-CMSTNO is switched-off), to the Hierarchical Risk Parity (HRP), Maximum Sharpe Ratio (MSR), Minimum Volatility portfolio (MVP) and a buy-and-hold strategy on the SPY exchange-traded fund. To check the robustness of our result, the comparison is achieved via a bootstrapping application, wherein $n = 30$ stocks are randomly selected (with replacement) out of the entire universe of stocks available in 10.000 iterations. In terms of weight stability and concentration, RS-CMSTNO, CMSTNO, and HRP produce more stable and better-diversified portfolios compared to MSR and MSV as measured by the portfolio turnover and the Hirschman–Herfindahl Index respectively. Moreover, our methodology outperforms competing methods in terms of risk-adjusted measures – namely Sharpe ratio, Sortino ratio, Information ratio, and Treynor ratio – on the back of larger portfolio returns only partially offset by higher portfolio standard deviation introduced by the equally weighting system in the first step of the optimization. Finally, the RS-CMSTNO achieves the lowest portfolio kurtosis, confirming its role as a successful hedging tool against tail risk events. We conclude that superior risk-adjusted returns are associated with shifting the allocation towards the peripheries through the regime-switching mechanism regulating the portfolio's eigenvector centrality.

A limitation of our study is the choice of the distance metric, which is insensible to the sign of the correlation coefficient. Future studies should explore the effects of different distance formulations that would factor-in the correlation's sign. Moreover, future work should focus on testing different tree approaches, centrality measures, and clustering methodologies. The methodology here implemented may also be tested on other asset classes or for other time frequencies.

Declaration of competing interest

The authors declare that they have no known competing financial interests or personal relationships that could have appeared to influence the work reported in this paper.

Data availability

Data will be made available on request.

Appendix A. List of the 100 US stocks used in this study

Name	Ticker	Name	Ticker
Apple	AAPL	Intel	INTC
Abbott Labs	ABT	Intuit	INTU
Accenture	ACN	Intuitive Surgical	ISRG
Adobe	ADBE	Illinois Tool Works	ITW
ADP	ADP	J&J	JNJ
AMD	AMD	JPMorgan	JPM
Amgen	AMGN	Coca-Cola	KO
American Tower	AMT	Eli Lilly	LLY
Amazon.com	AMZN	Lockheed Martin	LMT
Anthem	ANTM	Lowe's	LOW
Air Products	APD	Mastercard	MA
American Express	AXP	McDonald's	MCD
Boeing	BA	Mondelez	MDLZ
Bank of America	BAC	Medtronic	MDT
Becton Dickinson	BDX	3M	MMM
Booking	BKNG	Altria	MO
BlackRock	BLK	Merck&Co	MRK
Bristol-Myers Squibb	BMJ	Morgan Stanley	MS
Blackstone	BX	Microsoft	MSFT
Citigroup	C	NextEra Energy	NEE
Caterpillar	CAT	Netflix	NFLX
Crown Castle	CCI	Nike	NKE
Cigna	CI	NVIDIA	NVDA
Colgate-Palmolive	CL	Oracle	ORCL
Comcast	CMCSA	PepsiCo	PEP
Canadian National	CNI	Pfizer	PFE
Railway			
Costco	COST	Procter&Gamble	PG
Salesforce.com	CRM	Prologis	PLD
Cisco	CSCO	Qualcomm	QCOM
CSX	CSX	Raytheon Technologies	RTX
CVS Health Corp	CVS	RBC	RY
Chevron	CVX	Starbucks	SBUX
Dominion Energy	D	Charles Schwab	SCHW
Deere&Company	DE	Southern	SO
Danaher	DHR	S&P Global	SPGI
Walt Disney	DIS	Stryker	SYK
Duke Energy	DUK	AT&T	T
Estee Lauder	EL	Target	TGT
Ford	F	TJX	TJX
FedEx	FDX	Thermo Fisher Scientific	TMO
Fidelity National Info	FIS	T-Mobile US	TMUS
Fiserv	FISV	Texas Instruments	TXN
General Electric	GE	UBS Group	UBS
Gilead	GILD	UnitedHealth	UNH
General Mills	GIS	Union Pacific	UNP
Alphabet A	GOOGL	United Parcel Service	UPS
Goldman Sachs	GS	Verizon	VZ
Home Depot	HD	Wells Fargo&Co	WFC
Honeywell	HON	Walmart	WMT
IBM	IBM	Exxon Mobil	XOM

Appendix B. Low-volatility MST with tickers

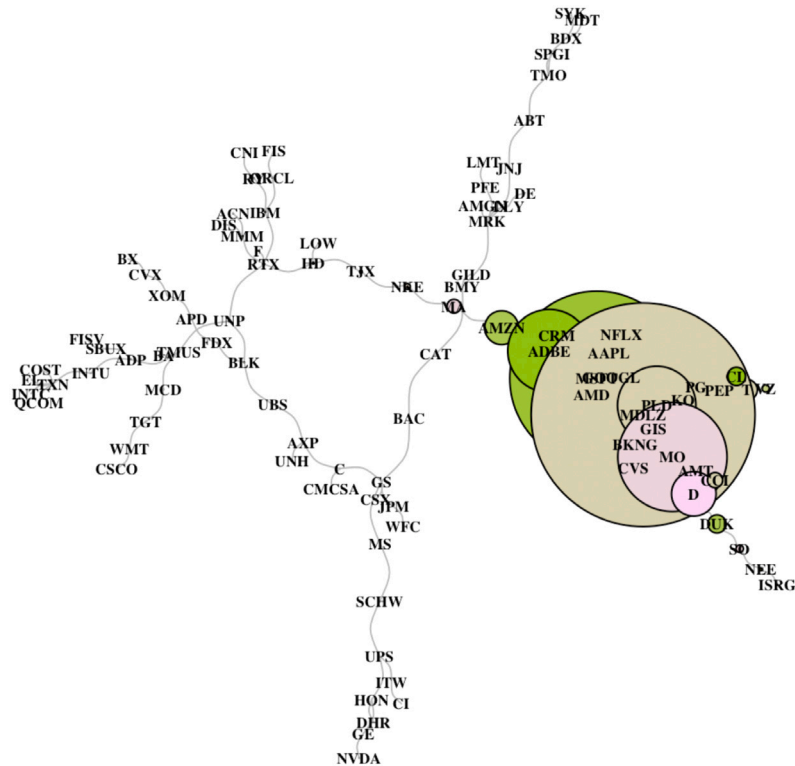


Fig. B.3. MST in low volatility regime.

Note: The MST representation of the 100 largest US securities by market cap as of December 2019 (when the regime detection model signaled a low volatility regime) including the tickers on each node.

References

- Andersen, T. G., Bollerslev, T., Diebold, F. X., & Labys, P. (2000). Great Realizations. *Risk*, 13, 105–108.
- Anderson, H., & Vahid, F. (1998). Testing multiple equation systems for common nonlinear components. *Journal of Econometrics*, 84(1), 1–36, URL: <https://EconPapers.repec.org/RePEc:eee:econom:v:84:y:1998:i:1:p:1-36>.
- Barndorff-Nielsen, O. E., Hansen, P. R., Lunde, A., & Shephard, N. (2006). Designing realized kernels to measure the ex post variation of equity prices in the presence of noise. *Econometrica*, 76(6), 1481–1536.
- Barndorff-Nielsen, O. E., & Shephard, N. (2004). Econometric Analysis of Realized Covariation: High Frequency Based Covariance, Regression, and Correlation in Financial Economics. *Econometrica*, 72, 885–925. <http://dx.doi.org/10.2139/ssrn.305583>.
- Billio, M., Getmansky, M., Lo, A. W., & Pelizzon, L. (2012). Econometric measures of connectedness and systemic risk in the finance and insurance sectors. *Journal of Financial Economics*, 104(3), 535–559.
- Black, F., & Litterman, R. (1992). Global portfolio optimization. *Financial Analysts Journal*, 48(5), 28–43.
- Bollobás, B. (1998a). *Graduate texts in mathematics: vol. 184, Modern graph theory. Vol. 2* (p. 4). New York NY: Springer.
- Bollobás, B. (1998b). Random graphs. In *Modern graph theory* (pp. 215–252). Springer.
- Bollobás, B. (2001). *Random graphs*. (73), Cambridge University Press.
- Bucci, A., & Ciciretti, V. (2022). Market regime detection via realized covariances. *Economic Modelling*, 111, Article 105832.
- Cho, J. S., & White, H. (2007). Testing for Regime Switching. *Econometrica*, 75(6), 1671–1720. <http://dx.doi.org/10.1111/j.1468-0262.2007.00809.x>, URL: <https://onlinelibrary.wiley.com/doi/abs/10.1111/j.1468-0262.2007.00809.x>.
- Clarke, R., De Silva, H., & Thorley, S. (2002). Portfolio constraints and the fundamental law of active management. *Financial Analysts Journal*, 58(5), 48–66.
- Davies, R. B. (1987). Hypothesis testing when a nuisance parameter is present only under the alternatives. *Biometrika*, 74(1), 33–43, URL: <http://www.jstor.org/stable/2336019>.
- De Pooter, M., Martens, M., & Van Dijk, D. (2008). Predicting the Daily Covariance Matrix for S&P 100 Stocks Using Intraday Data - But Which Frequency to Use? *Econometric Reviews*, 27, 199–229.
- DeMiguel, V., Nogales, F. J., & Uppal, R. (2014). Stock Return Serial Dependence and Out-of-Sample Portfolio Performance. *The Review of Financial Studies*, 27(4), 1031–1073. <http://dx.doi.org/10.1093/rfs/hhu002>, arXiv:https://academic.oup.com/rfs/article-pdf/27/4/1031/24449449/online_appendix.pdf.
- Hansen, B. E. (1992). The Likelihood Ratio Test Under Nonstandard Conditions: Testing the Markov Switching Model of GNP. *Journal of Applied Econometrics*, 7, S61–S82, URL: <http://www.jstor.org/stable/2284984>.
- Haugen, R. A., Talmor, E., & Torous, W. N. (1991). The effect of volatility changes on the level of stock prices and subsequent expected returns. *The Journal of Finance*, 46(3), 985–1007.
- Jobson, J. D., & Korkie, B. (1980). Estimation for Markowitz efficient portfolios. *Journal of the American Statistical Association*, 75(371), 544–554.
- Kaufman, L., & Rousseeuw, P. J. (1990). *Finding groups in data: an introduction to cluster analysis*. John Wiley.

- Kruskal, J. B. (1956). On the shortest spanning subtree of a graph and the traveling salesman problem. *Proceedings of the American Mathematical Society*, 7, 48–50.
- Ledoit, O., & Wolf, M. (2003). A Well-Conditioned Estimator for Large-Dimensional Covariance Matrices. *Journal of Multivariate Analysis*, 88(2), 365–411.
- Ledoit, O., & Wolf, M. (2004). Honey, I Shrunk the Sample Covariance Matrix. *The Journal of Portfolio Management*, 30(4), 110–119.
- Liu, Q. (2009). On Portfolio Optimization: How and When Do We Benefit from High-Frequency Data? *Journal of Applied Econometrics*, 24(4), 560–582, URL: <http://www.jstor.org/stable/40206292>.
- Lopez de Prado, M. (2016a). A Robust Estimator of the Efficient Frontier. Available at SSRN 3469961.
- Lopez de Prado, M. (2016b). Building portfolios that outperform out-of-sample. *The Journal of Portfolio Management*, 42(4), <http://dx.doi.org/10.3905/jpm.2016.42.4.059>.
- Mantegna, R. (1999). Hierarchical structure in financial markets. *The European Physical Journal B*, 11(1), 193–197. <http://dx.doi.org/10.1007/s100510050929>.
- Markowitz, H. (1952). Portfolio selection. *The Journal of Finance*, 7(1), 77–91. <http://dx.doi.org/10.2307/2975974>, URL: <https://www.jstor.org/stable/2975974>.
- Michaud, R. O. (1989). The Markowitz Optimization Enigma: Is 'Optimized' Optimal? *Financial Analysts Journal*, 45(1), 31–42. <http://dx.doi.org/10.2469/faj.v45.n1.31>.
- Onnela, J.-P., Chakraborti, A., Kaski, K., Kertesz, J., & Kanto, A. (2003). Dynamics of market correlations: Taxonomy and portfolio analysis. *Physical Review E*, 68(5), Article 056110.
- Papenbrock, J. (2011). *Asset clusters and asset networks in financial risk management and portfolio optimization* (Ph.D. thesis), Karlsruher Institut für Technologie (KIT).
- Patton, A. J. (2011). Volatility forecast comparison using imperfect volatility proxies. *Journal of Econometrics*, 160(1), 246–256.
- Peralta, G., & Zareei, A. (2016). A network approach to portfolio selection. *Journal of Empirical Finance*, 38, 157–180.
- Potters, M., Bouchaud, J.-P., & Laloux, L. (2005). Financial applications of random matrix theory: Old laces and new pieces. arXiv preprint Physics/0507111.
- Preis, T., Kenett, D. Y., Stanley, H. E., Helbing, D., & Ben-Jacob, E. (2012). Quantifying the behavior of stock correlations under market stress. *Scientific Reports*, 2(1), 1–5.
- Raffinot, T. (2017). Hierarchical clustering-based asset allocation. *The Journal of Portfolio Management*, 44(2), 89–99.
- Simon, H. A. (1991). The architecture of complexity. In *Facets of systems science* (pp. 457–476). Springer.
- Tibshirani, R., Walther, G., & Hastie, T. (2001). Estimating the number of clusters in a data set via the gap statistic. *Journal of the Royal Statistical Society. Series B. Statistical Methodology*, 63(2), 411–423.
- Výrost, T., Lyócsa, Š., & Baumöhl, E. (2019). Network-based asset allocation strategies. *The North American Journal of Economics and Finance*, 47, 516–536.
- Ward, J. H., Jr. (1963). Hierarchical grouping to optimize an objective function. *Journal of the American Statistical Association*, 58(301), 236–244.
- Zhou, B. (1996). High-Frequency Data and Volatility in Foreign-Exchange Rates. *Journal of Business & Economic Statistics*, 14(1), 45–52. <http://dx.doi.org/10.2307/1392098>, Full publication date: Jan., 1996.